



OPEN Low lying excited states quantum entanglement and continuous quantum phase transitions

Yan-Chao Li¹✉, Yuan-Hang Zhou¹, Yuan Zhang¹ & Hai-Qing Lin²

From the perspective of entanglement in low-lying excited states, a profound analysis was carried out regarding the quantum phase transitions within three models that fall outside the Landau-Ginzburg-Wilson (LGW) paradigm. In the context of the deconfined quantum critical point (DQCP) in a one-dimensional quantum spin chain, our findings demonstrate a tight correlation between the reconstruction of low-lying excitation spectra and the DQCP. The precise location of the critical point and its continuous nature can be signaled by the singular behaviors of the entanglement of the first-excited state. Moreover, in comparison with two types of Berezinskii-Kosterlitz-Thouless (BKT) phase transitions, the entanglement presents three different singularity characteristics. These characteristics not only unveil the essence of diverse symmetry types on either side of the DQCP but also expose the disparate causes underlying the formation of the two BKT type phase transitions.

Quantum phase transitions (QPTs), which are purely driven by quantum fluctuations, play a significant role in understanding the quantum mechanism behind many novel physical phenomena and are one of the central focuses in modern condensed matter physics^{1,2}. Traditionally, QPTs are well described by local order parameters and symmetry breaking theory within the Landau-Ginzburg-Wilson (LGW) paradigm. However, in recent years, researchers have found some new QPTs that cannot be classified into the category of LGW both in theory and experiments, such as topological QPTs^{3–6} and deconfined quantum critical points (DQCPs)^{7–10}. To incorporate these novel types of phase transitions into a unified theory, it is imperative to pursue fresh breakthroughs. As a unique characteristic of quantum systems, quantum entanglement has made important progress in the study of quantum phase transitions^{11–15}. Utilizing this pure quantum quantity to illuminate quantum phenomena is regarded as one of the feasible solutions.

The DQCP was originally introduced in two-dimensional (2D) quantum Heisenberg magnets, where a continuous QPT occurs between two quantum states with disparate symmetries^{7,8}. According to the LGW paradigm, when two symmetry-breaking phases of different types disrupt disparate symmetries, they conventionally experience transitions at two discrete and well-defined points. This invariably gives rise to an intermediate disordered or coexistent phase. Consequently, a direct continuous phase transition between such two symmetry-breaking phases is precluded under the conventional LGW framework. However, the discovery of this specific and anomalous phase transition seemingly challenges and breaks the confinement imposed by Landau theory. It is precisely due to this remarkable deviation that it is termed the deconfined quantum phase transition. This novel phenomenon has attracted considerable theoretical interest^{9,16–19}. Recently, the experimental demonstration of the existence of the field-induced DQCP at low temperatures through high-pressure nuclear magnetic resonance measurements on layered quantum magnet $SrCu_2(BO_3)_2$ has further piqued researchers' enthusiasm for DQCP studies¹⁰. However, the natural properties of the phase transition are still under debate, and the controversy over whether it is continuous or weakly-first order still remains.

Existing theoretical studies have primarily focused on the non-analytic behavior of ground state properties at the transition points^{11,18,20}. However, for continuous phase transitions, it is widely recognized that they are not solely determined by ground state properties, but also significantly influenced by the interplay between the ground state and low-lying excited states^{1,21,22}. It has even been proposed that the continuous quantum phase transition is primarily driven by the reconstruction of the excitation energy spectra²¹. Furthermore, in the $J_1 - J_2$ model, the continuous QPT can be more effectively captured by the quantum fidelity (QF) (see its definition in the next section) of the first excited state rather than the ground state²³. Consequently, it is imperative to delve into the nature of this phase transition from the perspectives of low-lying excited states and quantum entanglement.

¹Center of Materials Science and Optoelectronics Engineering, College of Materials Science and Opto-Electronic Technology, University of Chinese Academy of Sciences, Beijing 100049, China. ²Zhejiang Institute of Modern Physics and School of Physics, Zhejiang University, Hangzhou 310027, China. ✉email: ycli@ucas.ac.cn

Additionally, the Berezinskii-Kosterlitz-Thouless (BKT) type QPT was originally introduced to describe the proliferation of topological defects in the two-dimensional XY spin model^{24,25}. As there is no genuine long-range order, topological phase transitions cannot be characterized by local order parameters and fall outside the LGW paradigm of symmetry breaking. In one-dimensional (1D) quantum systems, the continuous QPT with infinite order and lacking a local order parameter is also known as the BKT-type QPT. Due to the long-range correlation length and exponentially close gap at the transition point²⁶, numerical investigations of the BKT phase transition from pure ground-state properties pose a challenge. This is because extremely large system sizes are required to avoid severe finite-size effects^{22,27–30}. Therefore, we investigate here if one could detect these BKT-type transitions by examining excited state entanglement metrics.

In this study, our primary focus is placed on probing the DQCP through the examination of quantum entanglement within the low-lying excited states. Three examples will be presented: a) DQCP, b) BKT-type QPT occurring between phases that possess the same broken symmetry but exhibit different symmetry axes, and c) BKT-type QPT between phases with order and disorder. Our objective is to carry out a comparative analysis of the behaviors manifested by excited state quantum entanglement during quantum phase transitions. This analysis endeavors to disclose the disparities and correlations between two types of QPTs that deviate from the theoretical framework of LGW symmetry breaking, notwithstanding their disparate origins. Moreover, by examining the singularity of E_j^e at the phase transition point, such as its continuity and the consistency of the curvature on both sides of the phase transition point, we explore the correspondence between phase transitions and quantum entanglement, and ultimately reveal the fundamental nature of the formation of the DQCP, i.e., the different symmetry-breaking patterns on both sides of the phase transition point, from the point of view of entanglement.

Models and method

The one-dimension analog of DQCP has been constructed in several systems^{31–35}. Among them, one of the most widely studied is a one-dimensional spin chain model, which we have named the NNNXZ model³¹. Its Hamiltonian can be written as

$$H = \sum_{j=1}^N \left(-J_x \sigma_j^x \sigma_{j+1}^x - J_z \sigma_j^z \sigma_{j+1}^z + K_x \sigma_j^x \sigma_{j+2}^x + K_z \sigma_j^z \sigma_{j+2}^z \right), \quad (1)$$

where σ_j^α ($\alpha = x, z$) are the Pauli matrices on site j and J_α and K_α describe the nearest-neighbor ferromagnetic and next-nearest-neighbor antiferromagnetic interactions, respectively. N is the number of spins in the chain. For comparison with the known results and simplicity, we fix $J_x = 1$ and $K_x = K_z = 1/2$, leaving the only driving parameter J_z . It has been pointed out by field theory that a direct continuous QPT occurs between two states with disparate symmetries: the spin-z ordered ferromagnetic phase (zFM) ($J_z \gg 1$) with breaking \mathbb{Z}_2 and the VBS phase ($J_z \sim 1$) with breaking translational symmetry^{20,31}. Consequently, it represents a DQCP that bears an analogy to the 2D counterpart mentioned in Sec. I: Both entail continuous quantum phase transitions between states with distinct symmetry breaking, which manifests similarities in crucial physical characteristics and conceptual aspects notwithstanding the dimensional disparities. Subsequent numerical computations provide additional reinforcement to the conclusion regarding the continuous QPT. Through finite-size scaling analysis of the order parameters and the quantum entanglement of the ground state, it is predicted that the critical point is located at approximately $J_z^c \approx 1.465$, as reported in^{11,18,20}.

However, it cannot be excluded that the phase transition may be weakly first-order due to possible deviations in finite-size scaling analysis or the accuracy of numerical methods. In fact, a tiny discontinuous jump in the order parameter near the critical point has been observed, although the authors attributed it to an artifact of the numerical matrix product state method^{18,19}. Given that continuous quantum phase transitions are often associated with excited states^{21–23}, as discussed in Sec. I, we approach this issue from the perspective of low-lying excited states, combining quantum information approaches: Analyze the nature of this phase transition through the level crossing of low excited states and the behavior of entanglement formation in the first excited state.

For the BKT-type QPT, we first consider the 1D spin XXZ model. The Hamiltonian is defined as follows:

$$H = \sum_j^N \sigma_j^x \sigma_{j+1}^x + \sigma_j^y \sigma_{j+1}^y + \Delta \sigma_j^z \sigma_{j+1}^z, \quad (2)$$

where Δ describes the anisotropy of the spin-spin interaction on the z direction, and σ_j^α and N have the same meaning in Eq. (1). It is well known^{29,36,37} that in the regime $-1 < \Delta < 1$ the model is in a critical phase displaying gapless excitations and power law correlations. For $\Delta > 1$ the model enters a phase with Ising-like antiferromagnetic phase and a nonzero gap. The isotropic antiferromagnetic point $\Delta = 1$ is a BKT transition point, which is described by a divergent correlation length but without true long-range order, and is not easy to be detected by quantum information and finite-size scaling approaches^{27–29,37}.

Another BKT-type QPT that is further considered is the transition at $J_2/J_1 \approx 0.241$ of the $J_1 - J_2$ model. The Hamiltonian reads as

$$H = \sum_{j=1}^N (\sigma_j \cdot \sigma_{j+1} + \lambda \sigma_j \cdot \sigma_{j+2}), \tag{3}$$

where λ describes the ratio between the next-nearest-neighbor interaction J_2 and the nearest-neighbor interaction J_1 . It is well known there is a BKT-type quantum phase transition at $\lambda_c \approx 0.241^{23}$. For $\lambda < \lambda_c$, it is a gapless spin fluid or Luttinger liquid phase. As $\lambda > \lambda_c$, the ground state changes into a spin-gapped dimerized phase^{38,39}. Similar to the study of DQCP, we investigate the relationship between excited states and phase transitions, emphasizing the link between these transitions and the entanglement of excited states. Furthermore, we conduct a comparative analysis with the case of DQCP.

The concept of entanglement has been successfully used in detecting QPTs in various systems^{11,13,14,40}. Here, we adopt the entanglement of formation (EOF) as the detector, which is defined as⁴⁰

$$E_f(\rho_{AB}) = -f(C_{\rho_{AB}}) \log_2 f(C_{\rho_{AB}}) - [1 - f(C_{\rho_{AB}})] \log_2 [1 - f(C_{\rho_{AB}})], \tag{4}$$

where ρ_{AB} is the reduced density matrix of two neighboring sites A and B in the spin chain. $f(C_{\rho_{AB}}) = (1 + \sqrt{1 - C_{\rho_{AB}}^2})/2$ is a monotonically increasing function of the concurrence $C_{\rho_{AB}}$ ⁴¹. $C_{\rho_{AB}} = \max\{0, \lambda_1 - \lambda_2 - \lambda_3 - \lambda_4\}$, where $\lambda_1, \lambda_2, \lambda_3$, and λ_4 are the square roots of the eigenvalues of $\rho_{AB} \tilde{\rho}_{AB}$ in descending order. $\tilde{\rho}_{AB} = (\sigma_A^y \otimes \sigma_B^y) \rho_{AB}^* (\sigma_A^y \otimes \sigma_B^y)$ is the time-reversed matrix of ρ_{AB} . ρ_{AB}^* is the complex conjugation of ρ_{AB} and σ^y is the y component of Pauli operator. We will analyze the reduced density matrices ρ_{AB} formed by the ground state wave function ψ_g and the first-excited state wave function ψ_e , respectively. The resulting $E_f(\rho_{AB})$ are accordingly denoted as E_f^g and E_f^e .

Another widely utilized detector for QPT study from the field of quantum information theory is the QF. It is defined as the overlap between two quantum states $\psi(\lambda)$ and $\psi(\lambda + \delta)$ as $F(\lambda, \delta) = |\langle \psi(\lambda) | \psi(\lambda + \delta) \rangle|$ ^{23,27,30,42–44}. Here, λ is a driving parameter, while δ is a small quantity. If λ and $\lambda + \delta$ fall into different quantum states due to the vastly distinct geometrical structures of these states in Hilbert space, the value of $F(\lambda, \delta)$ will deviate from 1, making it a suitable indicator for QPT. Similar to the case of E_f , if the first excited quantum state is used to calculate F , it is labeled as F_e . We will also conduct comparative analysis on EOF results using QF.

We use the numerical exact diagonalization (ED) techniques to conduct simulations on the spin systems with a size of up to $N = 24$. To mitigate the impact of the boundary, periodic boundary conditions are taken into account for the EOF and QF calculations. In order to minimize memory consumption, the Hamiltonian matrix only records non-zero matrix elements, and the diagonalization process is accomplished by utilizing the subroutines within the ARPACK library.

Results and discussions

A. DQCP in the NNNXZ model

For the 1D DQCP model, as expected, due to the continuity of the ground state at the critical point, the ground state fidelity F_g does not exhibit any singularity. However, the first excited state fidelity F_e with $\delta = 1.0 \times 10^{-4}$ shows a sudden drop and its position J_z^m moves to the critical point J_z^c as N increases (see Fig. 1a). It is clear that there is a size-scaling behavior for J_z^m . To further confirm this conclusion, we do the finite-size scaling analysis for J_z^m . As shown in Fig. 1b, the system-size dependent J_z^m linearly scales as $1/N^{1.5}$ with error less than

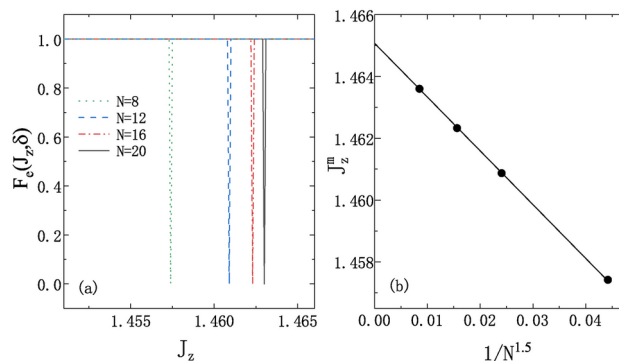


Fig. 1. (a) Fidelity of the first excited state $F_e(J_z, \delta)$ with $\delta = 1 \times 10^{-4}$ as a function of J_z under different system size N for DQCP model. (b) Linear finite-size scaling of the extrema J_z^m (black dots) of $F_e(J_z, \delta)$ in (a). When $N \rightarrow \infty$, the extrapolated critical value is $J_z^c = 1.4645(1)$.

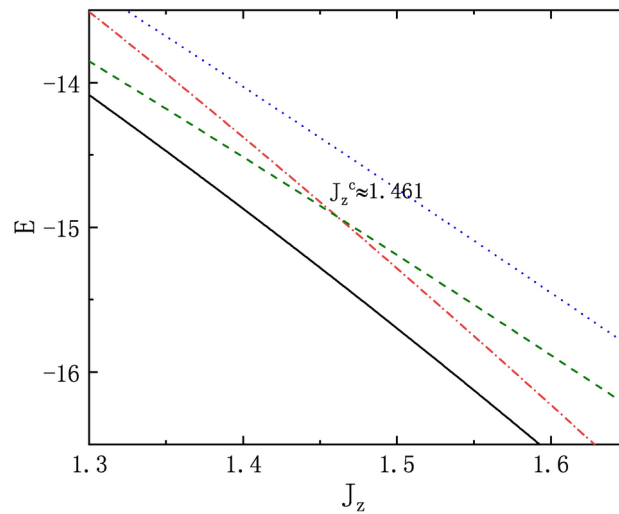


Fig. 2. Energy spectrum of the DQCP model with $N = 12$. There is a level crossing at $J_z \approx 1.461$ for the first excited state.

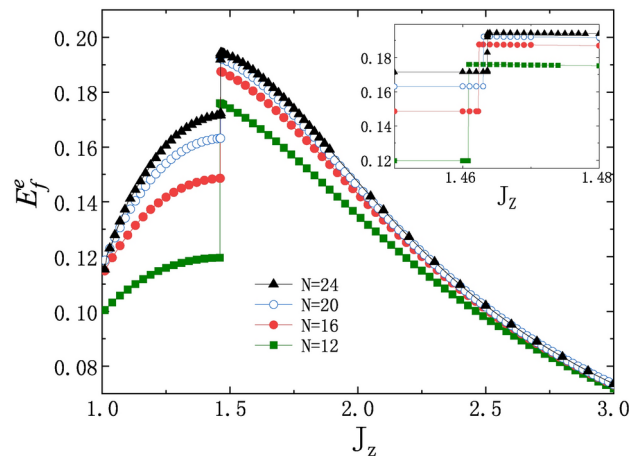


Fig. 3. (a) First excited state entanglement of formation E_f^e as a function of J_z under different N . The inset is an enlarged view of the curves near the jump for better clarity.

$\pm 1 \times 10^{-5}$. Here the linear scaling results were numerically obtained by power-law fitting. The extrapolated value to $N = \infty$ is $J_z^c \approx 1.4645(1)$, which is consistent with the best estimates results in Refs.^{11,18,20} very well.

Now we can confirm that the DQCP can be characterized by the first excited state fidelity. This is quite similar to the case of the $J_1 - J_2$ model in Ref.²³, where the continous QPT at $J_2 \approx 0.241$ can only be detected by the first excited state fidelity, but not the ground state fidelity. This means that the DQCP here should also be caused by the level crossing of low-excitation spectrum of the system. It is confirmed by the energy spectrums of the system for $N = 12$ as shown in Fig. 2, we can clearly see that the ground state is continuous while the first excited state is level crossing at $J_z \approx 1.461$. As pointed out in Ref.²¹, this originates from the energy level reorganization of the low-energy excited state reflects the continuous nature of the DQCP, from which we can rule out the possibility of this DQCP being a weakly first-order phase transition.

Now that both the DQCP and BKT-type transitions belong to the continuous category, and the dropping feature of the fidelity obviously cannot reflect their difference. How to identify their respective characteristic is still a problem. To deal with this issue we turn to the quantum entanglement. The first excited state entanglement of formation E_f^e as a function of J_z under different system size N is plotted in Fig. 3. A very remarkable phenomenon is the jump behavior of the curve near the phase transition point.

We discovered that the position of this jump point and its changes in relation to N (see the local enlarged view as an inset at the bottom of Fig. 3) align perfectly with the critical point behavior described by F_e . This indicates that EOF in the first excited state can clearly reflect this DQCP. Furthermore, E_f^e exhibits an intriguing characteristic: it attains a maximum on both sides of the jump point. This finding suggests that if the jump point indeed marks a critical point, then both quantum states reach their maximum entanglement at the phase transition point. Resembling its behavior at the BKT-type phase transition within the XXZ model (refer to the

subsequent discussion), the ground state entanglement of formation E_f^g , will display a maximum value in the vicinity of the phase transition point. The distinction lies in the fact that the position of its extreme value will vary with the system size N , and a particular scaling behavior exists, which is analogous to the extreme value behavior of E_f^e herein. Nevertheless, it will not exhibit a jumping behavior similar to that of E_f^e . Consequently, it is less distinct than E_f^e for the purpose of identifying the phase transition, and thus the corresponding results are not provided.

We think this phenomenon completely reflects the feature of the DQCP and can be explained as follows: The degree of symmetries of the VBS and zFM phases besides the critical point becomes higher as they approach the critical point, and the degree of entanglement is usually related to the symmetries of the system for a specific quantum state, leading to the maximal entanglement. This is quite similar to the entanglement behavior for the XXZ model pointed out in Ref.²². However, there are also differences: As mentioned in Sec. II, the quantum states located on different sides of the DQCP exhibit complete breakdown of symmetries that are unrelated to each other. Consequently, for the DQCP system, the entanglement difference between E_f^e on both sides of the phase transition point is substantial, featuring a distinct jump at the phase transition point. Furthermore, the entanglement gap $\Delta E_f^e = E_{f,R}^e - E_{f,L}^e$, where $E_{f,R}^e$ and $E_{f,L}^e$ are the E_f^e on the right and left sides of the jump point, respectively, follows a linear scaling with $1/N^{1.0}$ as shown in Fig. 4. It appears that the jump will not disappear even in the thermodynamic limit, reflecting the distinct quantum features of the quantum state beyond the critical point.

Nevertheless, it is noteworthy that the symmetries of the quantum states flanking the BKT transition point in the XXZ model pertain to the same category. At the phase transition point, both sides experience a transformation from $SU(2)$ to $SU_q(2)$ ²², with the sole distinction lying in the dominant direction. Symmetries of the same category are defined as those symmetries that harbor common mathematical properties and transformation traits within a particular symmetry group. Take, for instance, the spin symmetry \mathbb{Z}_2 and the spin \mathbb{Z}_3 symmetry previously mentioned. Both are intrinsically linked to the spin degree of freedom and govern the overall spin alignment within the system, thus falling into the same symmetry category. In contrast, translational symmetry is markedly different. It dictates the invariability of space, guaranteeing that the spatial configuration of the system preserves its fundamental characteristics under specific translation maneuvers. Consequently, translational symmetry and spin symmetry belong to disparate symmetry categories. Based on these considerations, we deduce that the entanglement of the first excited state in the XXZ model ought to be continuous at the phase transition point.

B. BKT-type QPT in the XXZ model

Figure 5 shows the behavior of the first excited state entanglement E_f^e as a function of Δ under different system sizes for the XXZ model. Although there is a level crossing in the first excited state at $\Delta = 1$ ²², E_f^e is indeed continuous and shows a round peak at the transition point as we expected. It has been pointed out that the ground state entanglement shows a maximum behavior and can be used to detect the BKT-type transition⁴⁵, and it is explained that it is the influence from the low-lying excited state to the ground state that causes the maximum behavior. Here, we note that the first excited state, as described in Ref.²¹, lies at the core of this ongoing transition. Entanglement on this state can serve as a straightforward indicator of the transition's occurrence. In fact, as shown in Fig. 5a, the peak values for the entanglement of the ground and first excited states decrease and increase, respectively, as N increases. It appears that they will converge into a single curve. The finite-size scaling behavior of E_f^e and E_f^g at the critical point $\Delta = 1$ supports this observation (see Fig. 5b): both of them follow a linear scaling behavior with $1/N^{2.0}$. As N approaches infinity, both of them approach the same value of approximately 0.238, indicating that the entanglement behavior of the ground and first excited states will tend

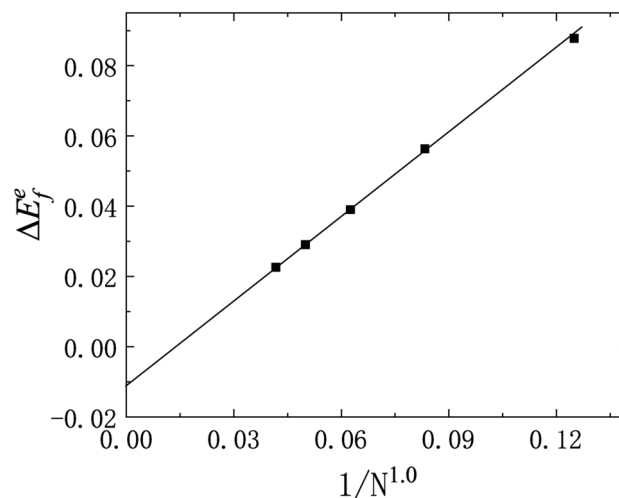


Fig. 4. (a) Finite-size scaling of the entanglement gap ΔE_f^e versus $1/N^{1.0}$. The black line is a linear fit, which indicates that the gap will not disappear in the thermodynamic limit.

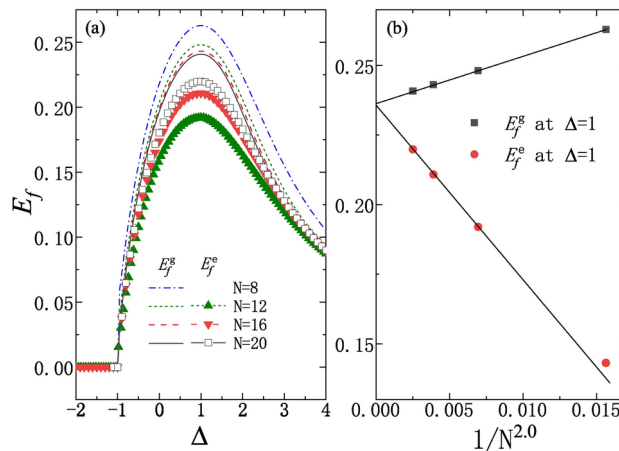


Fig. 5. (a) First excited state EOF E_f^e (with symbols) and ground-state EOF E_f^g (without symbols) as a function of Δ for different system size N in the XXZ model. (b) Linear finite-size scaling of E_f^g (black squares) and E_f^e (red dots) at the critical point $\Delta = 1$. In the thermodynamic limit E_f^e and E_f^g will approach the same value.

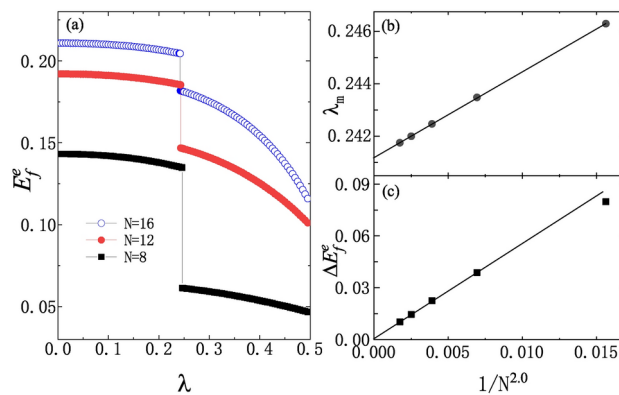


Fig. 6. (a) First excited state EOF E_f^e as a function of λ for different system size N in the $J_1 - J_2$ model. Linear finite-size scalings of (b) the jump position λ_m and (c) the entanglement gap ΔE_f^e beside the jump as a function of $1/N^{2.0}$. The critical point is extrapolated to be $\lambda_c = 0.2412(0)$, and the entanglement gap disappears in the thermodynamic limit.

to agree in the thermodynamic limit. This fully reflects the important role played by the low-excited states in the formation of such continuous quantum phase transitions.

C. BKT-type QPT in the $J_1 - J_2$ model

We then consider the BKT-type QPT in the $J_1 - J_2$ model for a further comparison. The first excited state entanglement E_f^e under different N is shown in Fig. 6a. Although there is no maximum behavior, there is a jump that moves towards the critical point as N increases. The jump position λ_m scales linearly with $1/N^{2.0}$ as shown in Fig. 6b, indicating the critical point $\lambda_c \approx 0.2412(0)$ in the limit of $N \rightarrow \infty$. It is evident that the scaling behavior of the jump in E_f^e and the sudden drop in fidelity (reported in Ref.²³) are consistent. This consistency illustrates that the jump observed here also reflects the level crossing in the first excited state and can be utilized to detect the continuous QPT.

The behavior of E_f^e differs from that in both the DQCP and XXZ models: there is no maximum phenomenon, and although it exhibits a jump similar to that in the DQCP model, it will disappear in the thermodynamic limit, as shown in Fig. 6c. The linear scaling relationship between the gap before and after the jump, ΔE_f^e , and $1/N^{2.0}$ indicates that ΔE_f^e disappears as N approaches infinity. We believe that the main reason for this is still related to the specific symmetry in the system. Unlike the DQCP with disparate symmetry breaking and the XXZ model with the same kind of symmetry breaking, only one-side symmetry breaking occurs for the dimerized state. As the driving parameter λ increases, the spin frustrated effect is enhanced, and the translational symmetry is gradually decreasing. However, due to the fact that these two phases belong to the same symmetry category, there is no jump for E_f^e in the thermodynamic limit, just as it is observed in the XXZ model. Furthermore, for a finite-size system, E_f^e does not exhibit a jump at the BKT phase transition of the XXZ model. We suggest that this

Model(QPT)	Continuity	Continuity ISL	Extremum	Symmetry
XXZ($\Delta = 1$)	Yes	Yes	Yes	$SU(2)$ to $SU_q(2)$
J_1 - J_2 ($J_2 \simeq 0.2416$)	No	Yes	No	Spin disorder to spin order
DQCP($J_z \simeq 1.4645$)	No	No	Yes	Translation symmetry to \mathbb{Z}_2

Table 1. Basic features of the first-excited state EOF E_f^e near the QPTs of the models, such as the continuity, continuity in the thermodynamic limit (ISL), and the symmetry of quantum states before and after the phase transition point.

phase transition is solely caused by anisotropy, which is not linked to system size like translation symmetry, but rather depends solely on spin direction. Consequently, there is no size scaling behavior and no jump behavior. Finally, the manifestation forms of the entanglement formed by the first excited state near the phase transition points of the three models are listed in Table 1 for comparison.

Summary

In summary, we have delved into the DQCP and BKT-type QPTs by examining the entanglement of low-lying excited states. Our findings indicate that the DQCP is triggered by the level crossing of the first excited state, much like the BKT-type QPTs, confirming its continuous nature. Through finite-size scaling analysis, we have identified the first excited state EOF E_f^e as a valuable tool for detecting these continuous QPTs. Furthermore, we observed that the curvature of E_f^e near the critical point offers insights into the symmetry properties of the phases beyond this juncture. Notably, disparate symmetry breaking results in a jump in E_f^e for the DQCP model, whereas the BKT-type QPT exhibits no such jump behavior in the thermodynamic limit, as states within the same symmetry category remain unaltered.

Although our conclusion is solely drawn from analyzing the most widely studied one-dimensional spin chain model, the phase transition point location in our analysis of small-size system precisely coincides with that from infinite-size system simulations in existing literature. The entanglement formation behavior in the first excited state also conforms to the known features of the DQCP. Thus, we infer that the DQCP of this model results from a level crossing between the first and second excited states. Whether such crossings always occur in the general DQCP as well as the general BKT-type QPTs, further research and verification are essential. However, at a minimum, we have provided a potential approach herein.

Data availability

All data generated or analysed during this study are included in this published article.

Received: 6 August 2024; Accepted: 11 February 2025

Published online: 21 February 2025

References

- Sachdev, S. *Quantum phase transition* (Cambridge University Press, Cambridge, U.K., 2011).
- Zeng, B., Chen, X., Zhou, D. L. & Wen, X. G. *Quantum information meets Quantum matter* (Springer, New York, 2019).
- Tsui, D. C., Stormer, H. L. & Gossard, A. C. Two-dimensional magnetotransport in the extreme quantum limit. *Phys. Rev. Lett.* **48**, 1559 (1982).
- Hasan, M. Z. & Kane, C. L. Colloquium: topological insulators. *Rev. Mod. Phys.* **82**, 3045 (2010).
- Qi, X. L. & Zhang, S. C. Topological insulators and superconductors. *Rev. Mod. Phys.* **83**, 1057 (2011).
- Hu, Z. et al. Evidence of the Berezinskii-Kosterlitz-Thouless phase in a frustrated magnet. *Nat. Commun.* **11**, 5631 (2020).
- Senthil, T., Vishwanath, A., Balents, L., Sachdev, S. & Fisher, M. P. A. Deconfined quantum critical points. *Science* **303**, 1490 (2004).
- Senthil, T., Balents, L., Sachdev, S., Vishwanath, A. & Fisher, M. P. A. Quantum criticality beyond the Landau-Ginzburg-Wilson paradigm. *Phys. Rev. B* **70**, 144407 (2004).
- Shao, H., Guo, W. & Sandvik, A. W. Quantum criticality with two length scales. *Science* **352**, 213 (2016).
- Cui, Y. et al. Proximate deconfined quantum critical point in $SrCu_2(BO_3)_2$. *Science* **380**, 1179 (2023).
- Yang, S. & Xu, J. B. Quantum entanglement and criticality in a one-dimensional deconfined quantum critical point. *Phys. Rev. E* **104**, 064121 (2021).
- Legeza, Ö. & Sólyom, J. Two-site entropy and quantum phase transitions in low-dimensional models. *Phys. Rev. Lett.* **96**, 116401 (2006).
- Berkovits, R. Entanglement properties and quantum phases for a fermionic disordered one-dimensional wire with attractive interactions. *Phys. Rev. Lett.* **115**, 206401 (2015).
- Osterloh, A., Amico, L., Falci, G. & Fazio, R. Scaling of entanglement close to a quantum phase transition. *Nature* **416**, 608 (2002).
- Gu, S. J., Deng, S. S., Li, Y. Q. & Lin, H. Q. Entanglement and quantum phase transition in the extended Hubbard model. *Phys. Rev. Lett.* **93**, 086402 (2004).
- Sandvik, A. W. Continuous quantum phase transition between an antiferromagnet and a valence-bond solid in two dimensions: evidence for logarithmic corrections to scaling. *Phys. Rev. Lett.* **104**, 177201 (2010).
- Chen, K. et al. Deconfined criticality flow in the Heisenberg model with ring-exchange interactions. *Phys. Rev. Lett.* **110**, 185701 (2013).
- Huang, R. Z., Lu, D. C., You, Y. Z., Meng, Z. Y. & Xiang, T. Emergent symmetry and conserved current at a one-dimensional incarnation of deconfined quantum critical point. *Phys. Rev. B* **100**, 125137 (2019).
- Roberts, B., Jiang, S. & Motrunich, O. I. Deconfined quantum critical point in one dimension. *Phys. Rev. B* **99**, 165143 (2019).
- Luo, Q., Zhao, J. & Wang, X. Intrinsic jump character of first-order quantum phase transitions. *Phys. Rev. B* **100**, 121111(R) (2019).
- Tian, G. S. & Lin, H. Q. Excited-state level crossing and quantum phase transition in one-dimensional correlated fermion models. *Phys. Rev. B* **67**, 245105 (2003).

22. Gu, S. J., Tian, G. S. & Lin, H. Q. Pairwise entanglement and quantum phase transitions in spin systems. *Chin. Phys. Lett.* **24**, 2737 (2007).
23. Chen, S., Wang, L., Gu, S. J. & Wang, Y. Fidelity and quantum phase transition for the Heisenberg chain with next-nearest-neighbor interaction. *Phys. Rev. E* **76**, 061108 (2007).
24. Berezinskii, V. Destruction of long-range order in one-dimensional and two-dimensional systems having a continuous symmetry group I. *Class. Syst. Sov. Phys. JETP* **32**, 493 (1971).
25. Kosterlitz, J. M. & Thouless, D. J. Ordering, metastability and phase transitions in two-dimensional systems. *J. Phys. C: Solid State Phys.* **6**, 1181 (1973).
26. Itzykson, C. & Drouffe, J. M. *Statistical Field Theory* Cambridge University Press. Cambridge, U.K. (1989).
27. Sun, G., Kolezhuk, A. K. & Vekua, T. Fidelity at Berezinskii-Kosterlitz-Thouless quantum phase transitions. *Phys. Rev. B* **91**, 014418 (2015).
28. Lv, C. P., Li, Y. C. & Lin, H. Q. Robust approach to study the effect on quantum phase transitions of various perturbations at finite temperatures. *Phys. Rev. B* **105**, 054424 (2022).
29. Chen, S., Wang, L., Hao, Y. & Wang, Y. Intrinsic relation between ground-state fidelity and the characterization of a quantum phase transition. *Phys. Rev. A* **77**, 032111 (2008).
30. You, W. L., Li, Y. W. & Gu, S. J. Fidelity, dynamic structure factor, and susceptibility in critical phenomena. *Phys. Rev. E* **76**, 022101 (2007).
31. Jiang, S. & Motrunich, O. Ising ferromagnet to valence bond solid transition in a one-dimensional spin chain: Analogies to deconfined quantum critical points. *Phys. Rev. B* **99**, 075103 (2019).
32. Sandvik, A. W., Balents, L. & Campbell, D. K. Ground state phases of the half-filled one-dimensional extended Hubbard model. *Phys. Rev. Lett.* **92**, 236401 (2004).
33. Weber, M., Parisen Toldin, F. & Hohenadler, M. Competing orders and unconventional criticality in the Su-Schrieffer-Heeger model. *Phys. Rev. Res.* **2**, 023013 (2020).
34. Ogino, T., Kaneko, R., Morita, S., Furukawa, S. & Kawashima, N. Continuous phase transition between Néel and valence bond solid phases in a J-Q-like spin ladder system. *Phys. Rev. B* **103**, 085117 (2021).
35. Mudry, C., Furusaki, A., Morimoto, T. & Hikihara, T. Quantum phase transitions beyond Landau-Ginzburg theory in one-dimensional space revisited. *Phys. Rev. B* **99**, 205153 (2019).
36. Gogolin, A. O., Nersisyan, A. A. & Tsvetlik, A. M. *Bosonization approach to strongly correlated systems* (Cambridge University Press, Cambridge, England, 1999).
37. Campos Venuti, L. & Zanardi, P. Quantum critical scaling of the geometric tensors. *Phys. Rev. Lett.* **99**, 095701 (2007).
38. Castilla, G., Chakravarty, S. & Emery, V. J. Quantum magnetism of CuGeO_3 . *Phys. Rev. Lett.* **75**, 1823 (1995).
39. Okamoto, K. & Nomura, K. Fluid-dimer critical point in $S = 1/2$ antiferromagnetic Heisenberg chain with next nearest neighbor interactions. *Phys. Lett. A* **169**, 433 (1992).
40. Werlang, T., Trippé, C., Ribeiro, G. A. P. & Rigolin, G. Quantum correlations in spin chains at finite temperatures and Quantum Phase Transitions. *Phys. Rev. Lett.* **105**, 095702 (2010).
41. Wootters, W. K. Entanglement of formation of an arbitrary state of two qubits. *Phys. Rev. Lett.* **80**, 2245 (1998).
42. Gu, S. J. Fidelity approach to quantum phase transitions. *Int. J. Mod. Phys. B* **24**, 4371 (2010).
43. Zanardi, P. & Paunković, N. Ground state overlap and quantum phase transitions. *Phys. Rev. E* **74**, 031123 (2006).
44. Zanardi, P., Quan, H. T., Wang, X. G. & Sun, C. P. Mixed-state fidelity and quantum criticality at finite temperature. *Phys. Rev. A* **75**, 032109 (2007).
45. Wang, L., Shinaoka, H. & Troyer, M. Fidelity susceptibility perspective on the Kondo effect and impurity quantum phase transitions. *Phys. Rev. Lett.* **115**, 236601 (2015).

Acknowledgements

We acknowledge financial support from the National Natural Science Foundation of China (Grants No. 12074376 and No. 52072365), the Beijing Municipal Natural Science Foundation (Grants No.1222027), and the NSAF (Grants No. U1930402).

Author contributions

Hai-Qing Lin provided a lot of discussions and suggestions. Yan-Chao Li wrote the main manuscript text and Yuan-Hang Zhou and Yuan Zhang participated in numerical calculations and figures preparation. All authors reviewed the manuscript.

Declarations

Competing interests

The authors declare no competing interests.

Additional information

Correspondence and requests for materials should be addressed to Y.-C.L.

Reprints and permissions information is available at www.nature.com/reprints.

Publisher's note Springer Nature remains neutral with regard to jurisdictional claims in published maps and institutional affiliations.

Open Access This article is licensed under a Creative Commons Attribution-NonCommercial-NoDerivatives 4.0 International License, which permits any non-commercial use, sharing, distribution and reproduction in any medium or format, as long as you give appropriate credit to the original author(s) and the source, provide a link to the Creative Commons licence, and indicate if you modified the licensed material. You do not have permission under this licence to share adapted material derived from this article or parts of it. The images or other third party material in this article are included in the article's Creative Commons licence, unless indicated otherwise in a credit line to the material. If material is not included in the article's Creative Commons licence and your intended use is not permitted by statutory regulation or exceeds the permitted use, you will need to obtain permission directly from the copyright holder. To view a copy of this licence, visit <http://creativecommons.org/licenses/by-nc-nd/4.0/>.

© The Author(s) 2025